



1975-INTS-INTS  
FR7700865  
3K2

**EIGHTH WORLD CONFERENCE  
ON NONDESTRUCTIVE TESTING.**  
*Cannes France, 6-11 September 1976*  
**HUITIÈME CONFÉRENCE MONDIALE  
SUR LES ESSAIS NON DESTRUCTIFS**

A TECHNIQUE FOR THE DECONVOLUTION OF THE PULSE SHAPE OF ACOUSTIC EMISSION SIGNALS BACK TO THE GENERATING DEFECT SOURCE

UNE TECHNIQUE POUR LA DÉCONVOLUTION DE L'IMAGE DES IMPULSIONS DE L'ÉMISSION ACOUSTIQUE, AU DÉFAUT GÉNÉRATEUR.

HOUGHTON, J.R./PACKMAN, P.F. TOWNSEND, M.A.

Nashville, Tennessee

Tennessee State University/Vanderbilt Univ.

U.S.A.

**SUMMARY:** Acoustic emission signals recorded after passage thru the instrumentation system can be deconvoluted to produce signal traces indicative of those at the generating source, and these traces can be used to identify characteristics of the source.

**RESUME :** Les signes d'émission acoustique enregistrés après leur passage par l'instrumentation, peuvent être déconvolutés pour produire des traces des signes indicatives de ceux émis par la source génératrice: et ces traces peuvent s'employer pour identifier certaines caractéristiques de la source.

## I. INTRODUCTION

Researchers are continually developing new methods for increasing the range of applications of acoustic emissions, e.g., in the fields of flaw detection, indirect mechanical measurements of fluid flow and monitoring the performance of rotating equipment. Present acoustic emission emphasis has been directed toward the understanding of pulse generation during the propagation of material defects. The equipment, electrical techniques and associated science can easily be extended to the study of acoustic pulses produced by other types of generating mechanisms, i.e., wear of ball bearing surfaces and loose particulate detection.

The initiation and propagation of the defect within the structure or specimen is accompanied by the sudden release of energy. This strain energy released has been correlated with the stress field of the crack, and the local stress intensity factor at crack propagation. This strain energy is composed of two parts, the elastic strain energy associated with the formation of new crack surfaces, and the strain energy associated with the formation of the plastic zone of deformation in the immediate vicinity of the crack tip. This energy released propagates spherically from the defect in the form of an elastic wave, whose characteristics are those associated with normal elastic wave propagation.

Additional acoustic within the metallic structure can be associated with stress waves from metallurgical transformations, e.g., martensitic transformations within heat treated steels. Here the transformation that occurs is accompanied by an acoustic burst associated with the release of energy by shear displacements. Additionally in aluminum alloys; fracture of the nonmetallic inclusions or cracking of intermetallics would also lead to acoustic bursts. In the case of structural components, sources of acoustic noise are associated with the slipping of bolted or riveted connections. These exhibit slip-stick frictional interface acoustic bursts. Thus detection of crack related acoustic signals from within structures also subjected to machinery noise, bearing noise and noise associated with heating and cooling stresses is a rather significant problem.

The state of the art in acoustic emission can be divided into roughly three major areas: (1) fundamental studies about the mechanism of acoustic emission sources

## ACOUSTIC EMISSION DECONVOLUTION

(2) applied studies of the relationship between acoustic signals and the mechanical integrity of the specimen or structure and (3) applications programs seeking to utilize acoustic emission studies for inservice inspection of completed structures. The applications studies on acoustic emission can be further subdivided into several sub classes: pulse counting, frequency analysis of signals and rise time analysis.

Much of the research today in acoustic emission nondestructive testing is in counting pulses emanating from a source. All pulses whose amplitude is greater than some preselected baseline signal level are counted as a function of time. Either the total number of pulses or the pulse rate is used as one variable, and stress or strain and/or some other mechanical variable are recorded to get a characteristic curve. A family of such characteristic curves is collected and judged for the influence of the variable under investigation, such as load or specimen geometry. The acoustic emission measurement systems used for pulse counting measurements have been optimized via laboratory experience to have the following range of characteristics:

- 1) Natural frequency: Between 100 and 500 KHz, primarily because of the good transmission through the material of the pulse information in this frequency range.
- 2) Transducer damping: Low for extended periods of ringing  
 $\zeta = 0.01$
- 3) Filtering: High-pass for frequencies above 50 KHz in order to mask out unwanted low frequency background noise.

Recent studies [1-4] have been conducted to analyze the frequency spectra of AE signals in metals and nonmetals. Beattie [2] suggests and this paper confirms that the acoustic emission pulse contains much more information than has been extracted by conventional ring-down counting analysis and that more refined signal processing techniques can be applied to the pulse to obtain additional information about the nature of the source.

Rise time analysis measures the time for the initial signal from the acoustic emission transducer to climb from a preselected signal height to a maximum. It is hoped that the rate of rise of the signal would be a measure of the severity or type of defect within the structure. The major difficulty in this area is the dispersion factors associated with the structure, and the contribution of the transducer characteristics to the measurement.

The pulse spectrum technique described in this paper is the result of a study of the applications of acoustic emission pulse signature analysis to the Space Shuttle nondestructive testing program of the National Aeronautics and Space Administration, NASA. Frequency spectrum analysis has been used by Graham and Alers [1] and others to study isolated AE events in simple structures with some successes. But when the analysis is carried over to inservice inspection of complex structures, the individuality of the AE signal from an incipient failure is lost in a host of other sources of AE signals which originate from benign sources. The work done for NASA examines the influence of the narrow frequency range available from commercially available AE equipment on the pulse shape and frequency spectrum. A time domain deconvolution technique is presented as a means for effectively removing the dynamic influence of the measurement system on the pulse shape.

### II. ANALYTICAL PULSES-Frequency Spectra and Deconvolution

A computer study was conducted to determine how effective the available signature analysis methods are in segregating pulses of different shapes after they have passed through an acoustic emission transducer and filter measurement system. Since no adequate model was available to describe the dynamic behavior of an acoustic emission transducer, a simple single degree of freedom model of an accelerometer was used for the computer model. Filters in the measuring system are modeled as single pole passive high-pass filter and low-pass filter. The system is shown in Figure 1.

## ACOUSTIC EMISSION DECONVOLUTION

The pulse shapes, representative of what pulse analysis methods must be able to distinguish, are the triangle, cosine and square. The criteria for judging the accuracy of each pulse analysis method is how well each method identified differences in the pulse shapes.

The Fourier transform of a pulse is the most common means for characterization of a signature in both destructive and nondestructive testing. The advantage of this frequency transform is that it can treat one unique pulse. Samples of the Fourier spectra that are generated by a square, triangular and cosine pulse of duration  $T_p$  are identified as  $Y_1$  in Figure 2. The Fourier spectrum magnitudes were normalized with respect to the size of the pulse by division of the Fourier magnitude by the absolute value of the area between the pulse and the zero line.

The signals of interest shown schematically in Figure 1 are  $Z_2$ , the transducer output;  $Z_4$ , the system output;  $Z_5$ , the reconstituted (deconvoluted) input to the transducer; and  $Z_6$ , the deconvoluted representation of the acoustic emission source. In operator form  $Z_4$  is given by

$$\frac{Z_4(t)}{Z_1(t)} = \frac{-K_{pu} \omega_{lp} \omega_n^2 D}{(D^2 + 2\zeta\omega_n D + \omega_n^2)(D + \omega_{hp})(D + \omega_{lp})} \quad (1)$$

where  $D = \text{operator for } d/dt$

$$\zeta = C/2\sqrt{KM}$$

$$\omega_n = \sqrt{K/M}, \text{ transducer natural frequency } (2\pi f_n)$$

$$\omega_{hp} = \text{corner frequency of first-order high-pass filter } (2\pi f_{hp})$$

$$\omega_{lp} = \text{corner frequency of first-order low-pass filter } (2\pi f_{lp})$$

$$K_{pu} = \text{the calibration constant of the transducer}$$

Several pulse shape configurations were used to demonstrate the influence of the measuring system on the pulse shape. Three samples of different shaped pulses of different shaped pulses of short pulse width are shown in Figure 2. The damping ratio for the transducer was 0.01, the high-pass filter corner was  $f_{hp}/f_n = 0.1$  and the low-pass filter corner was  $f_{lp}/f_n = 4.0$ . These are reasonably representative of present counting designs.

The pulse shapes that come out of the transducer filter system are shown as  $Z_4$  in Figure 2. The Fourier spectrum of each output signal  $Z_4$  was computed and are shown as  $Y_4$ . The Fourier spectrums for the input signals  $Z_1$  are shown as  $Y_1$  and are easily distinguishable from each other. The significant characteristics of the Fourier spectrums  $Y_1$  are modified until they are indistinguishable by passage of the pulse through the measuring system. The output signal traces for the square, triangle and cosine pulse have nearly the same shape and the same Fourier spectrum. Notice from the  $Y_4$  plots that the frequency of high energy is at the transducer natural frequency. Hence, it can be concluded that the transducer and filtration system presently used for AE pulse signature analysis are a major deterrent in the search for a unique signature from AE signals coming from defects.

This agrees with results presented by Graham and Alers [1]. They showed that the frequency analysis of signals associated with defect propagation was very similar in nature to the frequency analysis of signals obtained from "white noise" produced by grinding of small crystals on the end of the specimen. Ono and Ucisik [3] has also shown in a most recent study of the frequency analysis of signals associated with acoustic signals from cracks in aluminum alloys that the frequency response is more associated with the transducer characteristics than with the different alloys.

## ACOUSTIC EMISSION DECONVOLUTION

An alternative of frequency spectrum analysis is time domain reconstruction of the pulse trace. If the transducer and its modifying effects on the signal could be eliminated by computing the shape of the signal before it entered the transducer a major advance could be made in signal recognition. Then by holding the recorded output signal in a digital storage unit and feeding this information into the correct computer routine the signal can be deconvoluted\* to determine the approximate original shape of the pulse at the base of the transducer. To implement this approach equation (1) is expressed in suitable finite difference form:

$$\begin{aligned}
 Z_5(i) = & Z_5(i-1) - \frac{\Delta t}{K_{pu} \omega_n \omega_{hp} \omega_{Lp}} \left[ \omega_n^2 \omega_{hp} \omega_{Lp} Z_4(i) + \right. \\
 & + (\omega_n^2 \omega_{hp} + \omega_n^2 \omega_{Lp} + 2\zeta \omega_n \omega_{hp} \omega_{Lp}) (Z_4(i+1) - Z_4(i-1)) / 2 \Delta t \\
 & + (\omega_n^2 + 2\zeta \omega_n \omega_{Lp} + 2\zeta \omega_n \omega_{hp} + \omega_{hp} \omega_{Lp}) (Z_4(i+1) - 2Z_4(i) + Z_4(i-1)) / \Delta t^2 \\
 & + (2\zeta \omega_n + \omega_{hp} + \omega_{Lp}) (Z_4(i+2) - 2Z_4(i+1) + 2Z_4(i-1) - Z_4(i-2)) / 2 \Delta t^3 \\
 & \left. + (Z_4(i+2) - 4Z_4(i+1) + 6Z_4(i) - 4Z_4(i-1) - Z_4(i-2)) / \Delta t^4 \right] \quad (2)
 \end{aligned}$$

where  $i, i+1, \dots, i-1$ , etc. represent values at present, future and past discrete times.  $\Delta t$  is the sample period. The results,  $Z_5$  in Figure 2, is then the reshaped time-domain "pulse" based on the recorded output shape. The results compare favorably to the original signals that went into the transducer filter system. Thus, it appears that the deconvolution process can produce recognizable signals that are identical to the input signals and can effectively eliminate the signature identification difficulties caused by the measuring system.

---

\* Deconvolution is defined as identifying an input in the time domain, given the output and the system transfer function.

## III. EXPERIMENTAL PULSES - Deconvolution

Experimental studies of AE signals were measured with a Dunegan/Endevco Model D9202 acoustic emission pickup with amplifier and filter Dunegan/Endevco Model 2649 and the signals were recorded on an Ampex Corp PR 2200 tape recorder. The differential equation blocks used for the analysis of experimental data were similar to those shown in Figure 1 but the order of the differential equations for each unit were higher. For example the transducer model had two resonant frequencies, and the dynamic contribution of the tape recorder was included. An approximate model of the structure from the AE source to the transducer was developed from an analysis of the Fourier spectrums of the signal traces deconvoluted to the base of the transducer. The structural model selected for this present work had two resonant frequencies selected from the Fourier spectrum results. In the process of evolving the differential equation model for the experimental equipment, the equation went well past an eighth-order differential equation. The approach now is to deconvolute stage-by-stage through each component in turn. This modular approach makes it possible to change the model for each component as the component is switched for another or as a better model becomes available.

Several acoustic emission sources were used. There were (1) an acoustic pressure wave from a high energy spark discharge probe (2) the acoustic signals associated with a 1 gm steel ball impacting on a specimen surface, (3) propagation of ductile crack under increasing applied stress in an aluminum alloy and evaluation of the acoustic signals associated with a builtin defect within a ball bearing. In the case of the ball bearing artificial crack like defects were introduced into the rolling contact surface as well as into one of the balls.

In the case of the first three sources, care was taken to ensure that the specimen configuration was kept constant. In each case the acoustic source was located in the central region of a premachined compact tension specimen whose dimensions were approximately 100 x 100 x 12.5 mm. The location for the spark source and impact of the steel ball were chosen to be in the same area as the location of the fatigue crack. This was done so that the transfer function for the deconvolution associated with the specimen would remain essentially the same. Any mode conversion process associated with the propagation of the stress wave from the acoustic source would be identical for each of the tests.

For the initial program, three different transducers were used with the same acoustic generating source. Two series of tests were conducted, (1) multiple discharges of the spark source deconvoluted through the same transducer and (2) deconvolution of the spark source through different transducers. Analysis of the signals showed that the spark discharge acoustic emission burst could be reproduced successfully over a period of time. When using the same transducer and amplifying system, the deconvoluted traces were relatively similar, and could be identified as having been generated by the same source. When different transducers were used and the traces deconvoluted, it showed that the signals came from a similar source. This was possible even though the frequency response of the transducers were different. This showed that the deconvolution procedure was extremely powerful for signal analysis and that the characteristics of the transducer can be removed from the measuring system.

Figure 3a shows a deconvoluted signals associated with a spark discharge, Figure 3b shows the deconvoluted signals associated with the ball dropping, Figure 3c that of the crack propagation acoustic burst and Figure 3d the signals associated with the cut ball in the thrust ball bearing rotating under load. In all cases a Dunegan Endevco D9202 transducer was used. Figure 3a, 3b and 3c were measured in the same compact tensile specimen.

It should be noted that there is sufficient signal difference to differentiate between these different acoustic sources. Of particular interest is a comparison of the crack acoustic signals with that of the spark discharge. The rough similarity of these two signals indicates that the signal generated at the tip of the crack for a propagating aluminum crack is extremely short and pulse like in nature. The resemblance to a spark discharge is not too surprising since both sources are phenomenologically

## ACOUSTIC EMISSION DECONVOLUTION

similar. When the spark discharge occurs the voltage across the air gap is sufficient to break down the electrical resistance of the "air" gap. The energy is released in a burst, by propagation of the spark through the original nonconducting medium. The acoustic signals associated with the crack occur when the applied stresses (external energy source) is sufficiently high to destroy the bonding between the atoms of the material immediately ahead of the crack. At the onset of the failure of the material the crack propagates releasing the stress wave. If there were sufficient plastic deformation associated with the crack propagation, it could alter the time like shape.

The signals from the ball dropping on the plate indicate a slower release of energy than that associated with the crack propagation or the spark discharge. The ball drop location was on the surface, in a manner similar to the spark discharge, while the crack propagation occurred on both the surface and the interior. This may have resulted in some changes in the signal that were not considered.

These crack like signals are considerably different from those shown for the defect within the ball bearing. In this particular case, a electrical discharge machined slot was cut into one of the balls. Each time the bearing rotated in such a manner as to produce surface contact between the defective ball and the race, characteristic acoustic signals were developed. Acoustic signals are generated by "good" ball bearings also. The acoustic deconvolution of the acoustic emissions of good bearings shows characteristics similar to those of the bearings with artificial defects induced within the bearing. Additional techniques of signature analysis were developed to display the difference between ball bearing defects.

### IV. SUMMARY

Acoustic emission measurement techniques are examined and the transducer filter measurement system was identified to be a major factor in the results. Pulse counting methods and the associated ringing of the transducers can not be used to characterize and acoustic emission source. Frequency spectrum analysis of recorded acoustic emission signals will be significantly influenced by the resonant frequencies of the transducer and the mechanical structure. On the other hand, deconvolution of the recorded signals is possible when the system dynamic characteristics are defined. Experimental studies of acoustic signals from cracks growing and from noncrack related sources, i.e. ball dropping and running ball bearings with a defect, indicate that differentiation between sources is possible when deconvolution methods are used. This study shows the potential of a new signature analysis method for improving our understanding of acoustic emission phenomenon.

### REFERENCES

- (1). GRAHAM, L.J. and ALERS, G.A. "Spectrum analysis of acoustic emission in A533-B steel," Presented at ASNT Meeting, Los Angeles, 1973.
- (2). BEATTIE, A.G. "An analysis of the frequency and energy characteristics of acoustic emission signals from tensile and structural tests," SESA Spring Meeting, 1975, Chicago, Ill.
- (3). ONO, K. and UCISIK, J. "Acoustic emission behavior of aluminum alloys," Materials Evaluation ASNT, Feb. 1976, pp. 32-44.
- (4). LIPTAI, R.G., HARRIS, D.O., and TATRO, C.A. Acoustic Emission ASTM Special Technical Publication ASTM-STP 505 Philadelphia, Pa. 1972.

# ACOUSTIC EMISSION DECONVOLUTION

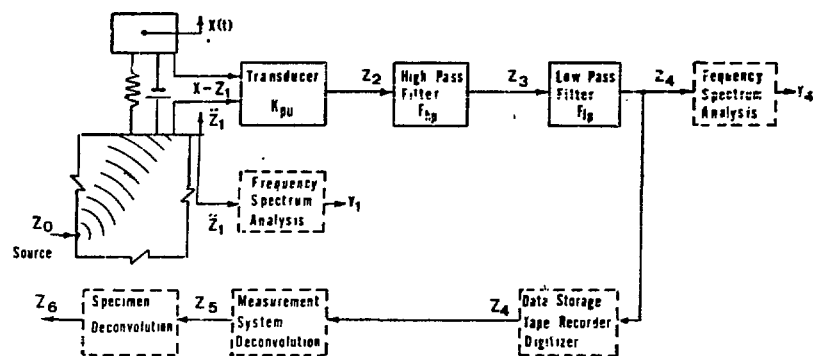


FIGURE 1 Schematic diagram of transducer, filter and recording system and deconvolution computational blocks.

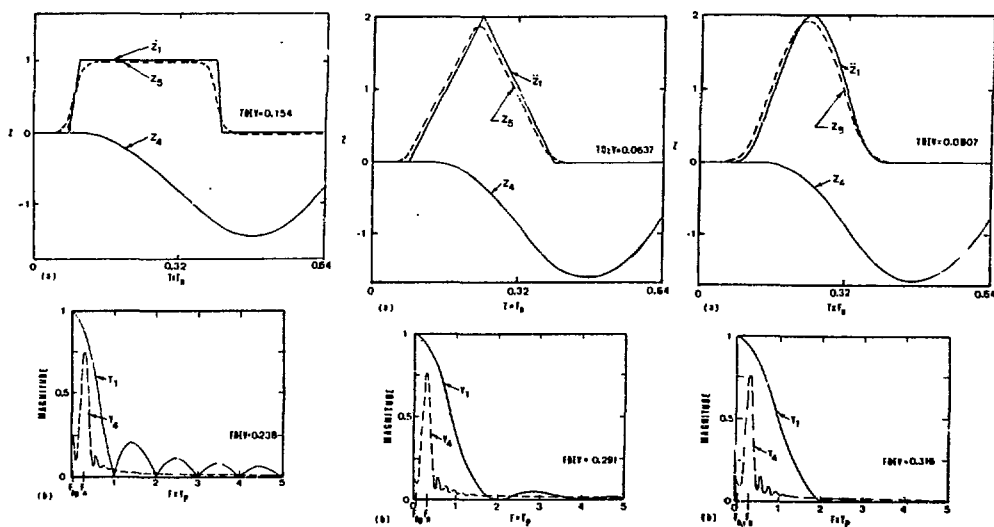


FIGURE 2 Analytical pulse signatures

ACOUSTIC EMISSION DECONVOLUTION

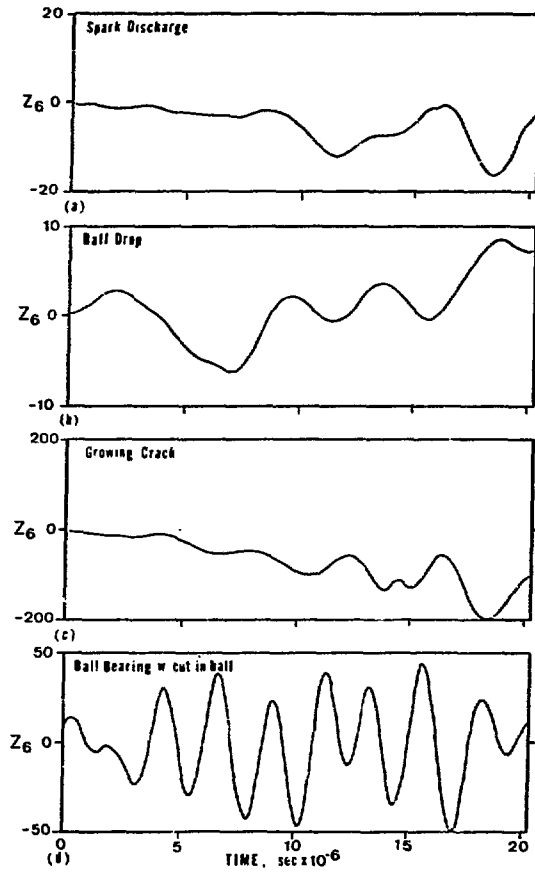


FIGURE 3 Deconvolution traces from experimental pulses.

